Catal Lett
DOI 10.1007/s10562-017-2120-7

Microwave-assisted Hydrothermal Fabrication of Magnetic Amino-grafted Graphene Oxide Nanocomposite as a Heterogeneous Knoevenagel Catalyst

Hassan M. A. Hassan[1,2] · Reda F. M. Elshaarawy[1,2] · Sandeep Kumar Dey[2] · Ilka Simon[2] · Christoph Janiak[2]

Received: 30 May 2017 / Accepted: 9 June 2017

Abstract A rapid and facile one-step microwave-assisted hydrothermal approach was developed for the synthesis of diethylenetriamine (DETA)-functionalized graphene oxide decorated with Fe_3O_4 nanoparticles. This DETA-modulated magnetic graphene oxide (Fe_3O_4@DETA@GO) was used as a heterogeneous base catalyst for the Knoevenagel condensation. The composite demonstrated outstanding catalytic performance with easy recovery and reusability.

Electronic supplementary material The online version of this article (doi:10.1007/s10562-017-2120-7) contains supplementary material, which is available to authorized users.

✉ Hassan M. A. Hassan
hassan.hassan@suezuniv.edu.eg

✉ Reda F. M. Elshaarawy
reda_elshaarawi@science.suez.edu.eg;
Reda.El-Shaarawy@uni-duesseldorf.de

Christoph Janiak
janiak@uni-duesseldorf.de

[1] Faculty of Science, Suez University, Suez, Egypt

[2] Institut für Anorganische Chemie und Strukturchemie, Heinrich-Heine Universität Düsseldorf, 40204 Düsseldorf, Germany

Published online: 22 June 2017

Graphical Abstract

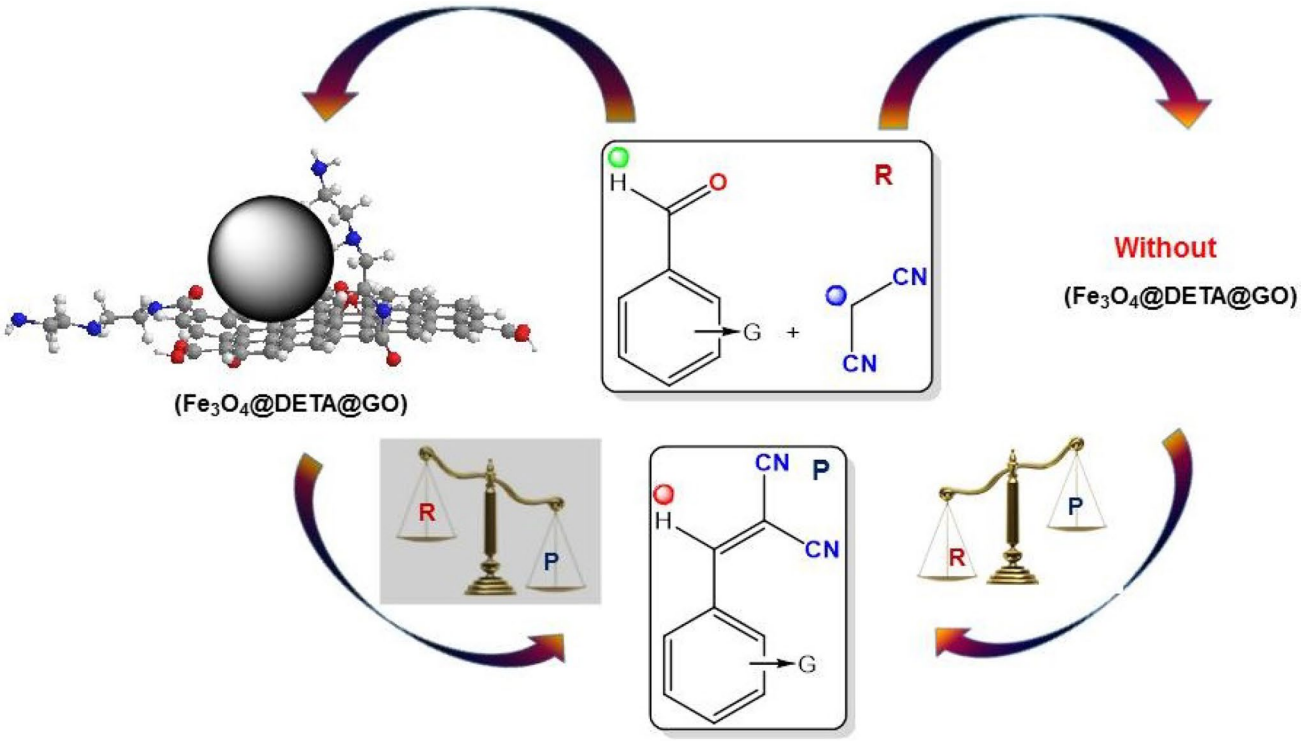

Keyword Graphene oxide · Magnetite nanoparticles · Amino-functionalization · Microwave-assisted hydrothermal · Knoevenagel reaction

1 Introduction

The Knoevenagel condensation, is a widely used reaction in organic chemistry for the synthesis of unsaturated carbonyl compounds. Due to its extended synthetic utility, a large number of reaction systems including solvent free and catalyst free ones have been developed for this reaction. However, most of the currently used methods catalyzed under homogeneous conditions and consequently the difficulty to reuse of the catalyst, high-power microwaves, long periods of reaction time and high reaction temperature are assigned for this approach. Recently, the applications of carbon-based nanomaterials (CBNs) in catalysis have been extensively grown in importance. Among various CBNs, graphene (G) is currently of high interest due to its unique structural, electronics characteristics [1], mechanical and thermal stability along with its large specific surface area and high adsorption capacity which offer many interesting applications [2–7]. These advantages recommend that graphene can be utilized as potential support for organic bases in different organic transformation reaction. Interestingly, the properties of single-layer graphene extend to bilayers and an oligo-layers graphene sheets [8]. Due to the π–π stacking of G sheets, the exploitation of monolayers of G in catalysis is challenging, therefore, an oligo-layered G is adopted in most catalytic applications. Graphene oxide (GO) sometimes also referred to "graphene" is prepared from natural graphite by the graphite oxidation process of Hummers and Offeman [9]. Structurally, GO bears epoxy, carbonyl, hydroxyl and carboxyl groups which gives it a weak acidic character ("graphitic acid"). This acidic nature is the main drawback limiting its catalytic applications in base-catalyzed processes. Therefore, functionalization of GO sheets can offer a novel opportunity for tailoring and developing robust, reusable catalysts [10–16]. Consequently, the grafting nitrogen atoms on the graphene matrix will induces surface basicity to GO. More examples of N-grafted nanocarbons as a basic catalyst can be identified with carbon nanotubes (CNTs) [17]. Bitter and his coworkers examined the Knoevenagel condensation between benzaldehyde and ethylcyanoacetate on the N-doped CNTs. It was found that the activity was controlled by the amount of pyridinic N components [17]. Tessonnier et al. [18] exploited amino-grafted CNTs as a solid basic catalyst for transesterification of glyceryl tributyrate with methanol and observed outstanding activity compared with the commercial hydrotalcite. An overview survey of the literature demonstrates that the use of N-incorporated graphene as a basic catalyst has been as yet constrained and importantly there is

still a lack of fundamental research into the working mechanism of graphene base catalysis. Amino-functionalized carbon-based materials were fabricated adopting various complicated approaches [14, 19]. Moreover, the prolonged Knoevenagel reaction time (1–4 h) is the major drawback for the previously few reported amine-functionalized GO catalysts [13, 20–22]. Thus, exploration facile protocol for fabrication of magnetically recoverable and extremely efficient amino-functionalized GO Knoevenagel catalyst is a valuable task. Herein, we report, a rapid and facile microwave approach for grafting GO with diethylenetriamine (DETA) along with decorating DETA@GO by magnetite nanoparticles to design Fe_3O_4@DETA@GO. The resulting composite combines heterogeneous GO with multiple basic amine sites and magnetite nanoparticles to overcome problems associated with the recovery of the base catalyst. Also the amine-grafting hinders the stacking of GO sheets by working as spacer. The amine-tagged magnetic nanocomposite (Fe_3O_4@DETA@GO) was used to catalyze the Knoevenagel reaction as a base-catalyzed process.

2 Experimental

Instrumentation, materials, preparation details and characterization data of Fe_3O_4@GO and Fe_3O_4@DETA@GO nanocomposites along with a general procedure for catalytic efficiency of Fe_3O_4@DETA@GO in Knoevenagel reaction can be found in the supporting information. Moreover, all ^{1}H NMR spectra for Knoevenagel products were reported, as well.

2.1 Synthesis of Catalysts

The Fe_3O_4@GO and Fe_3O_4@DETA@GO nanocomposites were fabricated by a facile one-step microwave-assisted hydrothermal approach (Scheme 1) in which, the magnetite nanoparticles (Fe_3O_4 NPs) was in situ prepared by a series consecutive reactions including alkaline hydrolysis of hydrated $FeCl_3$ in the presence of sodium acetate (NaOAc) to generate an amorphous ferrihydrite which further dehydrated to form crystalline FeO(OH) and partially reduced by ethylene glycol (EG) followed by a phase transformation producing magnetite NPs [23]. Thereafter the synthesized GO [24] was exfoliated by sonication in an EG dispersion containing the magnetite NPs without or with DETA. The mixture was then succumbed to hydrothermal–microwave treatment (details for the synthesis of the two composites are available in the supplementary data).

3 Results and Discussions

3.1 Structural Characteristics

As shown in Table S1, the nitrogen content of GO increased up to 1.14 wt% after amino-functionalization with DETA and simultaneous Fe_3O_4 deposition, indicating the successful immobilization of amine groups on the surface of GO.

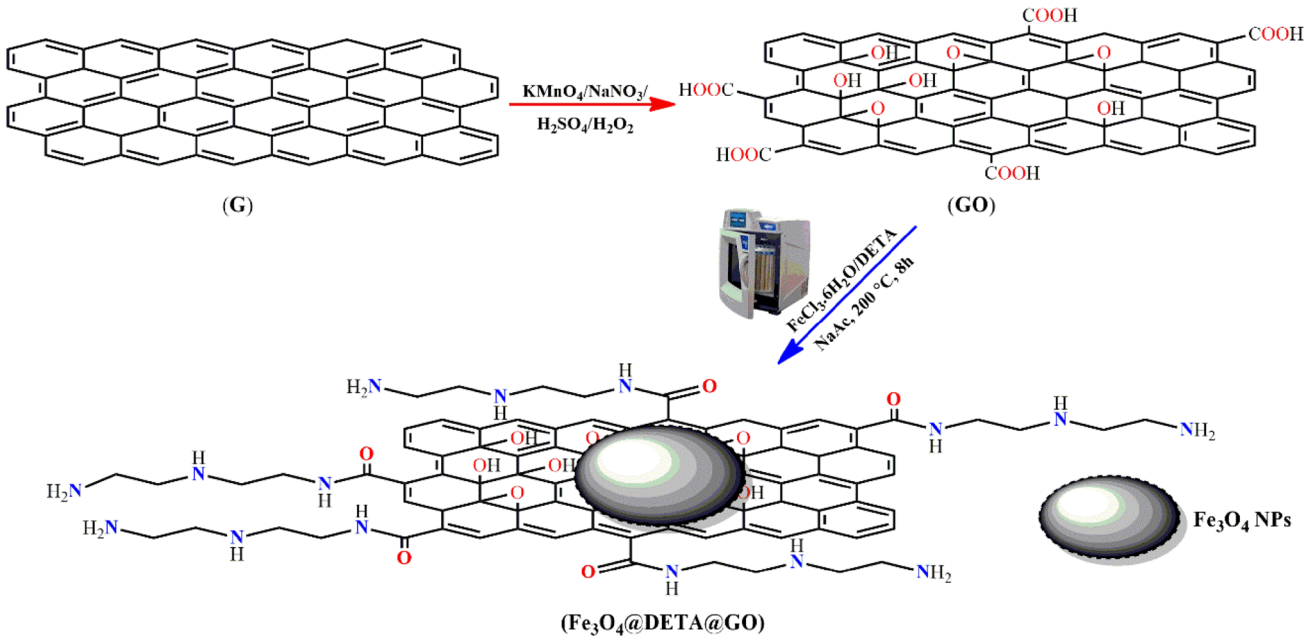

Scheme 1 Schematic illustration for the fabrication of Fe_3O_4@DETA@GO catalyst

Energy dispersive X-ray spectroscopic (EDX) analysis provides further evidence for our suggestion as revealed from the notice of peaks of O, C, Fe and N (Fig. S1, supplementary data).

The structural and surface properties of the Fe_3O_4@DETA@GO composite were characterized by powder X-ray diffraction (PXRD), Raman and X-ray photoelectron (XPS) spectrometry techniques (Fig. 1). As shown in Fig. S3, the changes in the powder X-ray diffractogram of Fe_3O_4@DETA@GO in comparison with that of Fe_3O_4@GO indicated that deposition of iron oxide nanoparticles on GO was significantly enhanced *via* the DETA functionalization. Without DETA an only low amount of iron oxide is deposited as revealed from the elemental analysis of Fe_3O_4@GO. Noteworthy, the disappearance of the peak at 10.89° (002) corresponding to GO sheets [24] indicates that the GO has been fully functionalized with Fe_3O_4@DETA nanocomposite. Interestingly that the crystalline peak at $2\theta \approx 33.5°$, characteristic for hematite (α-Fe_2O_3) phase, that observed in PXRD pattern of Fe_3O_4@GO was missed in Fe_3O_4@DETA@GO diffractogram confirming the reduction of hexagonal close-packed oxide (α-Fe_2O_3) into Fe_3O_4 spinel structure.

Raman spectra of Fe_3O_4/GO and Fe_3O_4/DETA-GO nanocomposites (Fig. 1a) show the D band (1345 and 1347 cm^{-1}), originating from the disordered carbon or *K*-point phonons of A_{1g} symmetry, and G band (1588 and 1601 cm^{-1}), corresponding to the E_{2g} mode of graphene and related to the vibration of sp^2-bonded C-atoms in a 2D hexagonal lattice, which are characteristic for GO sheet [14]. A red shift observed in the G band (by +3 cm^{-1}) of Fe_3O_4@DETA@GO in comparison to those of Fe_3O_4@GO confirms the successful functionalization of the graphenic network [14, 25]. The ratio D-band/ G-band of Fe_3O_4@DETA@GO becomes higher confirming the successful surface functionalization of GO by DETA which occurs *via* covalent attachment of amine mainly on the defect sites [26] as emphasized by the X-ray photoelectron spectra (XPS) in Fig. S4 (supplementary data) and Fig. 1b.

In the XPS of Fe_3O_4@DETA@GO deconvolution of the C1s profile (Fig. 1b) reveals the presence of a major peak at 284.6 eV (64%) corresponding to sp^2 bound graphenic carbon (C=C). Noteworthy three peaks of carbon attached to heteroatoms, namely C–N at 285.4 eV (15%), C–O at 286.2 eV (17%) and amide carbon in N–C=O at 288.3 eV (17%) are observed. Moreover, appearance of N1s peak at ~400 eV indicates the formation of C–N bond with secondary amide (O=C–NH–R), in accordance with previous literature. A slight shift in the C=O peak by $\Delta BE = +0.4$ eV, is due to conversion of carboxylic C=O into amide carbonyl, indicating that the functionalization of the GO mainly occurs through the carboxyl COOH groups to form –C(=O)–NH– amide bonds and the potent argument on the successful synthesis of the material.

The morphological features along with micro/nanostructure of the Fe_3O_4@DETA@GO nanocomposite was investigated by means of scanning electron microscopy (SEM) and high resolution transmittance electron microscopy (HRTEM), as depicted in Fig. 2. As shown in Fig. 2a and Fig. S5 (supplementary data), SEM micrograph of Fe_3O_4@DETA@GO revealed flak-like wrinkled graphene sheets with embedded tiny nanoparticles which can indexed to Fe_3O_4. EDX analysis (Fig. S1, supplementary data) shows the expected peaks for Fe metal (Fe-Lα, -Kα, -Kβ) besides

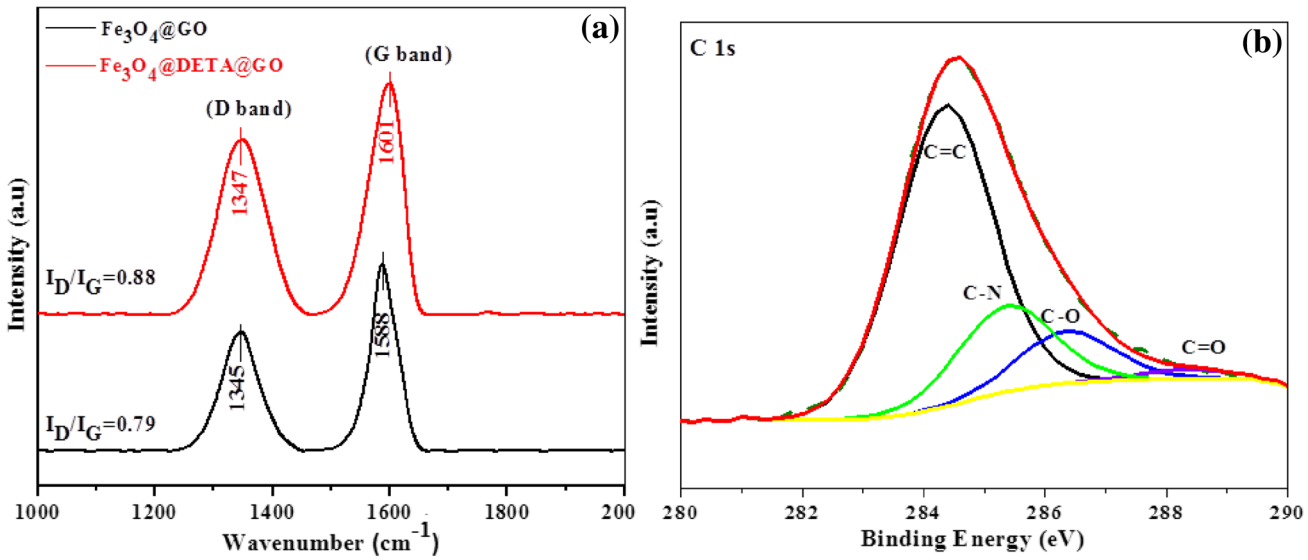

Fig. 1 **a** Raman spectra of Fe_3O_4@GO and Fe_3O_4@DETA@GO composites, **b** XPS of Fe_3O_4@DETA@GO composite

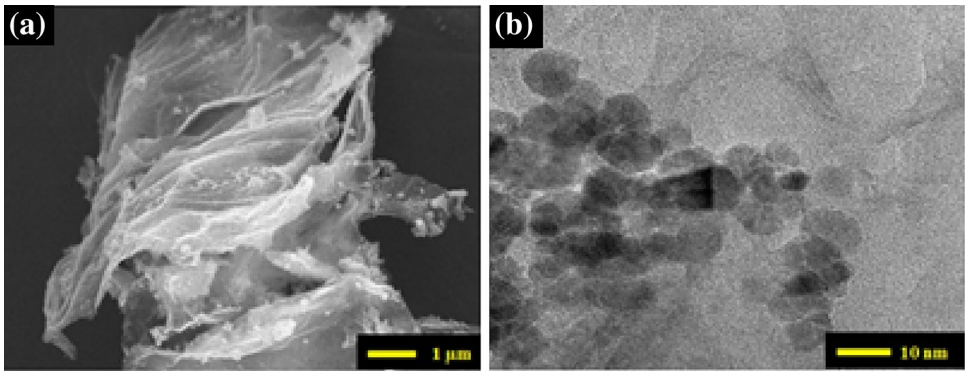

Fig. 2 **a** SEM image, **b** HRTEM image of the Fe_3O_4@DETA@GO nanocomposite

the peaks characteristic for carbon, oxygen and nitrogen of the GO and DETA. The HRTEM image of GO (Fig. S6, supplementary data) depicts the typical flake shape with some corrugations. On the other hand, HRTEM images of Fe_3O_4@DETA@GO nanocomposite (Fig. S6, 2b) show that the Fe_3O_4 as spherical NPs with a diameter of approximately 7 nm (Fig. 2b) on the surface of GO which was observed as wrinkled sheets with partial aggregation (Fig. S6). Additionally, trapezoidal crystals, typical of DETAs, were observed (Fig. 2b).

3.2 Catalytic Performance

To the best of our knowledge, amino-grafted GO decorated with magnetite nanoparticles has not been employed as a solid heterogeneous base for the catalysis of the Knoevenagel reaction. Inspired by these aforementioned facts and the low cost, ecofriendly and sustainable properties of amino-grafted GO, Fe_3O_4@DETA@GO has been examined as a solid base catalyst for the Knoevenagel reaction (Scheme 2).

The catalytic efficiency of Fe_3O_4@DETA@GO was assessed for the Knoevenagel condensation between 4-nitrobenzaldehyde with malononitrile in the presence of 2 mg of the nanocomposite in THF at 50 °C (Table 1). A control experiment in the absence of the catalyst was performed and only trace amounts of the desired product (4%) were observed at room temperature in THF within 1 h. Also increasing the temperature to 50 °C did not improve the yield of condensation product indicating that the reaction could not be carried out in the absence of the catalyst. Further, the reaction was performed in the presence of GO and the result revealed that GO exhibit only 20% conversion at the same optimum conditions. The model reaction has also been performed in the aprotic solvents such as toluene and ethyl acetate which also afforded quantitative conversion to the desired product within 30 min at 50 °C which showed 99% conversion for both. These observations suggested that aprotic solvents are generally adequate for catalyst assessment in the Knoevenagel reaction. To explore the substrate effect and generalize our catalytic system, the reactions between benzaldehyde or its derivatives with different steric and electronic characters with malononitrile were investigated under the given optimal conditions. In general, excellent conversions (92–99%) to the desired products were observed for most of the benzaldehyde derivatives carrying electron withdrawing groups (EWGs), except for 4-bromobenzaldehyde which yielded 62% of the desired product (Entry 7) (Table 1). However, benzaldehyde and its derivatives with electron donating groups (EDGs) give trace products, under the same reaction conditions The most plausible explanation for the reduced efficacy of our catalyst in case of benzaldehyde derivatives bearing EDGs is the mutual competition between ammonium moiety that capped the catalyst (electrostatically interact with malononitrile carboanion) and carbonyl group of aldehydic fragment (ion–dipole interact to malononitrile carboanion) which is responsible for the formation of final product, where the EDGs increase the electron density on the C-atom of carbonyl group causing reduced carboanion-carbonyl ion–dipole interaction and traces yield of final product, accordingly. Thus, the substrate scope of

Scheme 2 Schematic illustration for Knoevenagel condensation reaction

Table 1 Catalytic data of Fe_3O_4@DETA@GO catalyzed Knoevenagel condensation

Entry	R^1	R^2	Time (min)	Temp. (°C)	Yield (%)[a]	TON[b]
1	4-NO_2	CN[a]	30	50	99	619
2	3-NO_2	CN[a]	30	50	99	619
3	2-NO_2	CN[a]	30	50	99	619
4	4-CN	CN[a]	30	50	99	619
5	4-Cl	CN[a]	60	50	92	575
6	4-Br	CN[a]	60	50	62	388
7	H	CN[a]	60	50	55	297
8	CH_3	CN[a]	60	50	20	124
9	OCH_3	CN[a]	60	50	10	63
10	4-NO_2	COOMe[b]	60	50	20	125

General reaction condition: aldehyde (1.0 mmol), malononitrile (100 mg, 1.5 mmol) or methylcyanoacetate (150 mg, 1.5 mmol) in the presence of Fe_3O_4@DETA@GO (2 mg, N content 0.0016 mmol) in tetrahydrofuran at 50 °C

[a]Yields corresponding to aldehyde conversion are based on ^{1}H NMR analysis of the isolated product obtained (Fig. S11–S20, supplementary data)

[b]TON (turnover number) = moles of desired product formed/moles of catalyst (active center)

the Fe_3O_4@DETA@GO catalysed Knoevenagel reaction is limited to only for benzaldehyde derivatives with electron withdrawing groups, however with modest to high yields. The catalytic activity of the Fe_3O_4@DETA@GO has also been assessed in the Knoevenagel condensation of methylcyanoacetate with 4-nitrobenzaldehyde in THF at 50 °C. However, no significant yield has been obtained under the given reaction conditions (Table 1). Furthermore, turn over number (TON) measure the performance of catalyst. The TON values of different substituent are summarized in Table 1.

The exceptional catalytic efficacy of our new nanocomposite catalyst can be attributed to two main factors; (i) incorporation of Fe_3O_4 NPs which improve the loading of basic segment (DETA) on the surface of GO. (ii) Presence of multiple basic sites (thee N-atoms) in each DETA brush that facilitate the deprotonating of malononitrile and nucleophilic attack, accordingly (see Scheme 3).

The Knoevenagel condensation between 4-nitrobenzaldehyde and and malononitrile was selected as a module to assess the recyclability of the heterogeneous Fe_3O_4@DETA@GO nanocomposite under optimized reaction conditions. By the end of the reaction, the catalyst was recovered by magnetic separation, then washed with copious amounts of acetonitrile and air-dried. Thereafter, the catalyst was reused in the subsequent runs without further purification. As shown in Fig. 3a, the nanocomposite catalyst could be recovered and reused 5 cycles without significant loss of catalytic efficacy. These results confirm that the catalyst exhibited outstanding reusability and significant performance for Knoevenagel reaction along with infinitesimal leaching ratios of amine and Fe_3O_4 components and this give the catalyst promising in industrial scale. Additionally, in order to investigate the heterogeneous nature of the Knoevenagel reaction between 4-nitrobenzaldehyde and malononitrile using Fe_3O_4@DETA@GO as a solid base catalyst and that the measured overall activity was not owing to leached species, the hot filtration test (leaching experiment) was carried out (Fig. 3b). An experiment under the optimum condition was performed then, the reaction was stopped after 15 min of reaction, and the catalyst was removed from the reaction mixture by filtration, and the filtrate was allowed to continue the reaction under the same condition. The results revealed that no significant increase in the yield % after removal of Fe_3O_4@DETA@GO catalyst, definitely indicating that the anchored active centers were not leached out from the catalyst into the solution and the observed catalysis is truly heterogeneous on the catalyst surface.

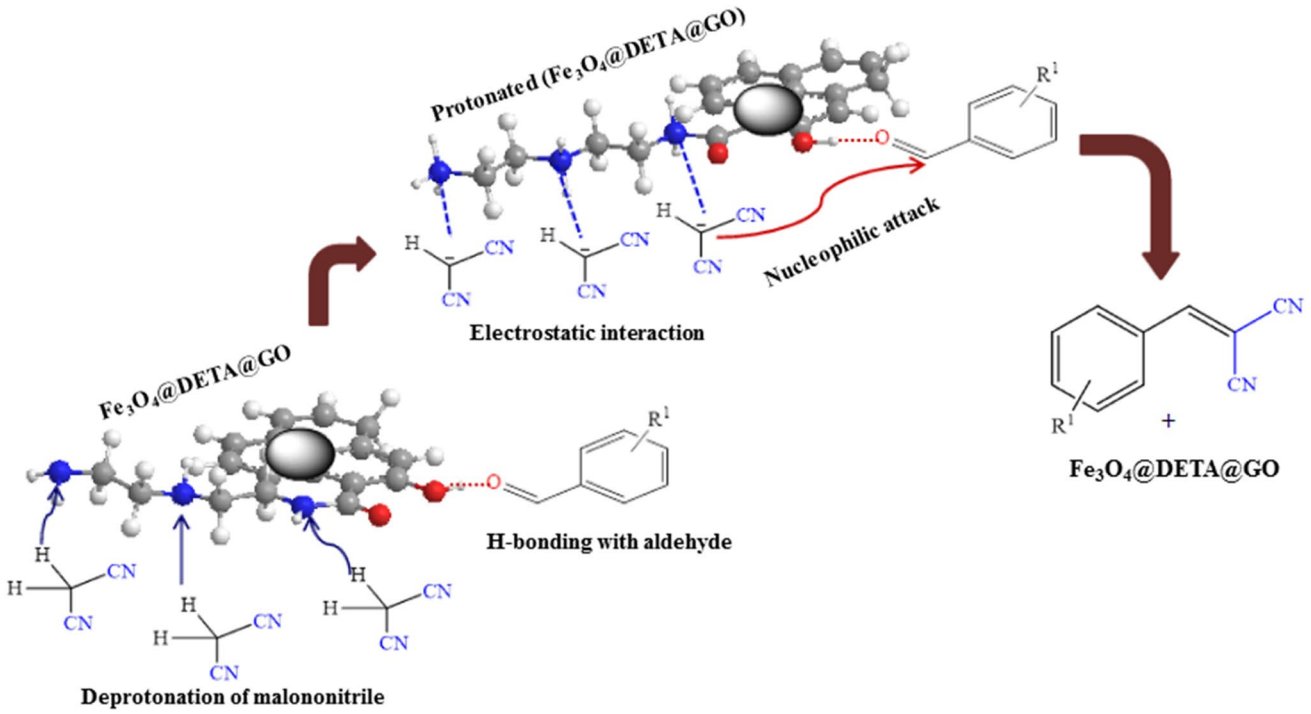

Scheme 3 A plausible mechanism for the Knoevenagel reaction of aldehydes and malononitrile catalyzed by Fe_3O_4@DETA@GO nanocomposite

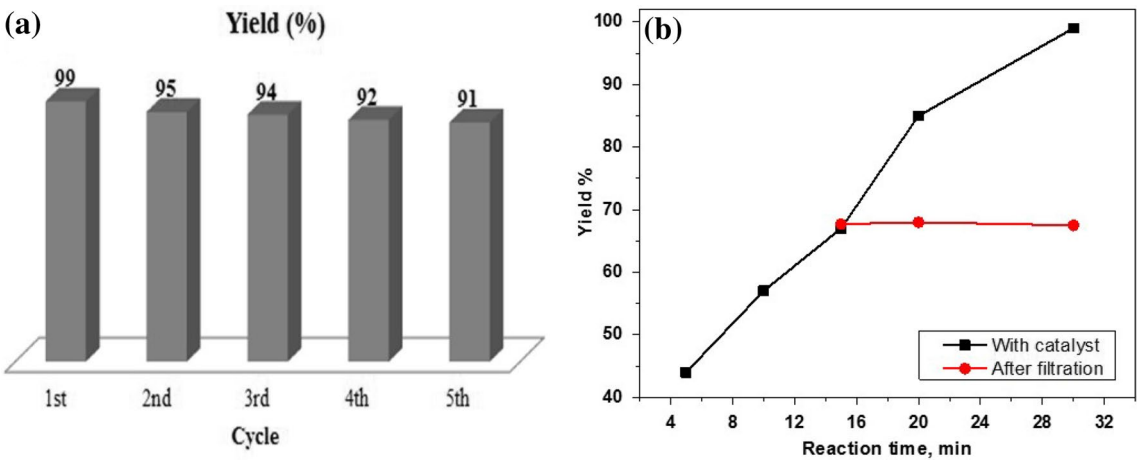

Fig. 3 **a** Recycling. **b** Hot filtration test of Fe_3O_4@DETA@GO nanocomposite catalyst for the Knoevenagel reaction between 4-nitrobenzaldehyde and malononitrile

4 Conclusion

In summary, we demonstrate a facile, scalable and a green one–step microwave-assisted hydrothermal method to fabricate a covalently attachment of amino moiety to GO using a top-down approach. The amino-grafted graphene oxide exhibited distinct catalytic efficiency and reusability in Knoevenagel condensation as a solid base catalyst.

References

1. Novoselov KS, Fal′ko VI, Colombo L, Gellert PR, Schwab MG, Kim K (2012) Nature 490:192–200
2. Marquardt D, Vollmer C, Thomann R, Steurer P, Mülhaupt R, Redel E, Janiak C (2011) Carbon 49:1326–1332
3. Zhang LL, Zhou R, Zhao XS (2010) J Mater Chem 20:5983–5992
4. Liu H, Ryu S, Chen Z, Steigerwald ML, Nuckolls C, Brus IE (2009) J Am Chem Soc 131:17099–17101

5. Esteban RM, Schütte K, Marquardt D, Barthel J, Beckert F, Mülhaupt C, Janiak C (2015) Nano-Struct Nano Object 2:28–34
6. Du J, Lai X, Yang N, Zhai J, Kisailus D, Su F, Wang D, Jiang L (2010) ACS Nano 5:590–596
7. Ling X, Xie L, Fang Y, Xu H, Zhang H, Kong J, Dresselhaus MS, Zhang J, Liu Z (2009) Nano Lett 10:553–561
8. Liang X, Chang ASP, Zhang Y, Harteneck BD, Choo H, Olynick DL, Cabrini S (2008) Nano Lett 8(5):1472–1476
9. Hummers WS, Offeman RE (1958) J Am Chem Soc 80:1339–1339
10. Jie H, Shunmin D, Weiming X, Yadan P, Shengjun D, Ning Z (2015) Catal Lett 145:1000–1007
11. Shunmin D, Xiaohui L, Weiming X, Mengmeng L, Yanan P, Jingwei H, Ning Z (2017) Catal Commun 92:5–9
12. Surjyakanta R, Sreekantha BJ (2017) Catal Commun 92:31–34
13. Rana S, Jonnalagadda SB (2017) Catal Commun 92:31–34
14. Bhaskar R, Joshi H, Sharma AK, Singh AK (2017) ACS Appl Mater Interfaces 9(3):2223–2231
15. Saptal VB, Sasaki T, Harada K, Nishio-Hamane D, Bhanage BM (2016) ChemSusChem 9(6):644–650
16. Zhang F, Jiang H, Li X, Wu X, Li H (2014) ACS Catal 4(2):394–401
17. Dommele S van, De Jong KP, Bitter JH (2006) Chem Commun 46:4859
18. Tessonnier JP, Villa A, Majoulet O, Suand DS, Schlögl R (2009) Angew Chem Int Ed 48:6543
19. Chen W, Yan L (2012) J Mater Chem 22:7456–7460
20. Sobhani S, Zarif F (2015) RSC Adv 5:96532–96538
21. Huang J, Ding S, Xiao W, Peng Y, Deng S, Zhang N (2015) Catal Lett 145(4):1000–1007
22. Xue B, Zhu J, Liu N, Li Y (2015) Catal Commun 64:105–109
23. Cha J, Lee S, Yoon SJ, Kim YK, Lee J-K (2013) RSC Adv 3:3631–3637
24. Hassan HMA, Abdelsayed V, Khder A-ES, AbouZeid KM, Terner J, El-Shall MS, Al-Resayes SI, El-Azhary AA (2009) J Mater Chem 19:3832–3837
25. Chakraborty S, Saha S, Dhanak VR, Biswas K, Barbezat M, Terrasid GP, Chakraborty AK (2016) RSC Adv 6:67916–67924
26. Machadoab BF, Serp P (2012) Catal Sci Technol 2:54–75